High Impedance Fault Localization in a Distribution Network using the Discrete Wavelet Transform

Mohd Syukri Ali[1], Ab Halim Abu Bakar[1], *Member IEEE,* Hazlie Mokhlis[1], *Member, IEEE,* Hamzah Aroff[2], Hazlee Azil Illias[1] and Muhammad Mohsin Aman[2], *Member IEEE*

***Abstract*--Basic guidelines for the preparation of a technical work for the Locating the faulty section for High Impedance Fault (HIF) in a power system is a major challenge especially for a radial distribution network. This is due to the effect of the complexity of the distribution network such as branches; non-homogenous lines and high impedance fault that results in a variation of fault location. In this paper, analysis of fault location using the discrete wavelet transform based Multi-Resolution Analysis (MRA) and database approach is proposed. The three-phase voltage signal at the main substation to be analyzed was measured. The 1st, 2nd and 3rd level of detail coefficients were extracted for each phase and were used for the identification of faulty section using the proposed method. The simulation on a 38 nodes distribution network system in a national grid in Malaysia using PSCAD software was simulated. The proposed method has successfully determined the faulty section.**

***Keywords*-- Discrete Wavelet Transform, Distribution Network, Fault localization, High Impedance Fault.**

I. Introduction

HIGH Impedance Fault (HIF) is a situation when an undesirable electrical contact is made between a conductor and non-conducting object. This type of fault condition exhibits the same arcing problem as a broken conductor lying on the ground. This arcing scenario may lead to potential hazards to both human life and environment. It also causes a fire hazards due to the arcing phenomenon. HIF could be successfully detected by utilizing the previous methods; however locating the fault is still the most challenging part. Identifying the exact or estimate fault location is necessary so that power restoration can be expedited, thus reducing the outage time and improving the system reliability [1-3].

Different HIF detection schemes have been proposed in the literature. Most of the detection schemes focus on identifying special features of the voltage and current signals associated with HIF. The irregularities in the voltage and current waveforms will give unique characteristics to be extracted. In order to extract useful features from these voltage and current signals, some signal processing methods have been utilized, such as Discrete Wavelet Transform [3], Fourier Transform [4], Prony Analysis [5], S-Transform [6], TT-Transform [7] and Phase Space Reconstruction [8].

Sarlak and Shahrtash [9] employed a multi-resolution morphological gradient (MMG) for features extraction of the current waveform. Sarlak and Shahrtash have also used the MMG method to distinguish HIF event from other phenomena such as capacitor bank switching, load switching and harmonic load. Nagy *et al.* have used the DWT to extract the voltage and current residuals to identify the faulty feeder. The faulty feeder is determined based on the power polarity [10]. Nagy *et al.* have also used the ratio of the residual current amplitude method to determine the faulty section. The measured highest ratio of residual current amplitude determines the faulty section [11].

In the present paper, classification of faulty section in a radial distribution network is done by utilizing discrete wavelet transform-based Multi-Resolution Analysis and a database approach. The proposed technique utilizes detailed coefficients of the 1st, 2nd and 3rd level resolutions that were obtained from the wavelet multi-resolution decomposition of a three-phase voltage signal. The proposed fault location method is also tested on a typical 38-nodes distribution network system in Malaysia. The simulation results were compared with the actual fault location to validate the proposed method.

II. Discrete Wavelet Transform Based Multi-Resolution Analysis

Wavelet is a mathematical function that satisfies certain mathematical requirements to represent the signal in time domain. The fundamental idea behind this is to analyze the signal according to scale, by dilation and translation. Discrete wavelet transforms (DWT)-based Multi-Resolution Analysis (MRA) is the extension from the DWT where the decomposition process was iterated with successive approximation components. DWT-based MRA splitting the

[1] Mohd Syukri Ali, Ab Halim Abu Bakar, Hazlie Mokhlis and Hazlee Azil Illias are working with University Malaya - Power Energy Dedicated Advance Center (UMPEDAC), Malaysia. They can be reached at mosba86@yahoo.com.my, a.halim@um.edu.my, hazli@um.edu.my, and h.illias@um.edu.my respectively.

[2] Hamzah Aroff and Muhammad Mohsin Aman are working with in Faculty Engineering University Malaya, Malaysia. They can be reached at ahamzah@um.edu.my and mohsinaman@siswa.um.edu.my respectively.

analyzed signal into many lower resolution levels until the individual detailed component consists of a single sample.

Using discrete wavelet transform (DWT) - based Multi-Resolution Analysis (MRA), wavelet coefficients are calculated based on the subset of scales and positions. The scales and positions are chosen based on power of two, called as *dyadic* scales and positions. In DWT, the original signal is decomposed by two complementary filters: high-pass filter and low-pass filters and emerges as two signals: high-frequency and low-frequency components. The low-frequency components of the signal are high-scaled decomposition, called as *approximations*. The high-frequency component is low-scale decomposition, called as *details*.

DWT-based MRA is a decomposition process that can be iterated with successive approximations to obtain more resolution levels. Fig. 1 shows the implementation of DWT-based MRA by using a bank of high pass filters, H and a low pass filters, L. The input signal, S, which propagates through the high pass and low pass filters is decomposed into low-pass component, c_m and high-pass component, d_m at each stage, where m=1, 2…., j. The scaling coefficients, c_m represents the approximation of the low-pass signal information and wavelet coefficients and d_m represents the detailed high–pass signal information.

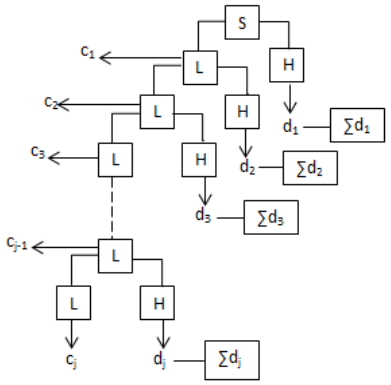

Fig. 1. Discrete Wavelet Transform based Multi-Resolution Analysis of Fault Signal (S).

Information extracted from the signal using DWT-based MRA is used to detect and identify various types of faults and to locate the faulty section in a distribution system network. For the faulty section, unique and useful information of voltage signals obtained can be analyzed using DWT-based MRA. For different faulty section, various pattern of voltage signal were created.

III. Proposed Method for the High Impedance Fault Location

In this paper, the classification of high impedance fault location algorithm is constructed based on the wavelet database. This section describes a distribution network, fault detection and classification, wavelet-based database system and ranking establishment.

A. Distribution Network

A schematic diagram of typical distribution network system in Malaysia consists of 38 nodes is shown in Fig. 2.

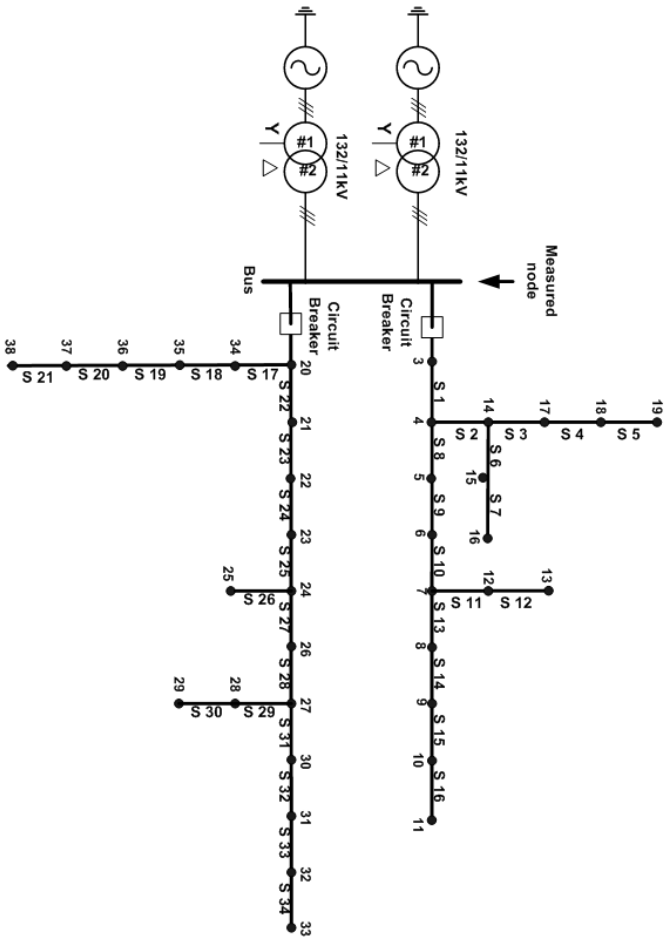

Fig. 2. Schematic Diagram of a Typical Distribution Network in Malaysia.

The system frequency is 50 Hz and the sampling frequency is 6.4 kHz, which produces 128 data samples for each cycle. The measurement is taken at feeder bus from a 132/11kV radial distribution network. The line data and cable parameter of the distribution network is given in the Appendix section I and II.

B. Fault Detection & Classification

For high impedance fault (HIF) detection and classification of fault location, 2 cycles of post disturbance of voltage signal are analyzed. Discrete wavelet transform of Daubechies 4th order, dB4 is used to observe the voltage signal.

HIF is detected when the detailed coefficient surge and give higher instantaneous fluctuation provides an easy means to identify an abnormality in the voltage signal as shown in Fig. 3(d). In order to classify the faulty section, the 1st, 2nd and 3rd level of the detailed signal of dB4 is analyzed and its summation of detailed coefficient is measured.

C. *Wavelet-Based Database System*

To generate a set of database, several high impedance fault (HIF) of 60Ω, 70Ω, 80Ω, 90Ω and 100Ω fault impedance are simulated at each node. The voltage signal obtained from the main feeder is decomposed using the DWT-based MRA to obtain the value of detailed coefficients for 2 cycles of post-disturbance event. Experimentally, it has been found that different impedance of fault generates a unique pattern of detailed coefficients at each node. The proposed average detailed coefficient, A_v between two neighboring nodes is calculated as a database for the particular section between the two nodes. A_v is calculated using Eqn. (1):

$$A_v = \frac{\sum d_i + \sum d_j}{2} \quad (1)$$

Where,

A_v = Average detailed coefficients between two nodes for phase A, B and C.

i and *j* is two adjacent node.

$\sum d_i$ = Summation of detailed coefficients for levels 1, 2 and 3 for nodes *i*

$\sum d_j$ = Summation of detailed coefficients for levels 1, 2 and 3 for node *j*

Five sets of database comprise of 60Ω, 70Ω, 80Ω, 90Ω and 100Ω fault impedance value is created. Each database for one section consists of 18 data of 1st, 2nd and 3rd levels of detailed coefficients for phases A, B and C of 1st and 2nd cycles of post-disturbance voltage waveform.

D. *Ranking Establishment*

The main objective of the work is to locate the faulty section. This is obtained by calculating the proposed *average of absolute difference* (AAD) between the faulted signal and database, using Eqn. (2).

$$AAD = \frac{\sum_{i=1}^{n} \left| \sum d_{i(measured)} - A_v \right|}{n} \quad (2)$$

Where

n= number of data (here *n*=18).

The faulty section is determined by finding the smallest value of AAD from all sections. The signal will be compared with all five databases for each section. Then, the ranking is made from the lowest to the highest value of AAD. This is done because in some cases, there will be an error in locating the faulty section from the first rank due to the topology of a radial network. This is because of the influence of radial topology that results in variation of faulty location. Thus, the second lowest AAD value will be considered as a faulty section until the real faulty section has been traced.

IV. Simulation and Results

The simulation has been performed to create a database and the proposed algorithm is tested with three different values of high impedance fault, 75Ω, 85Ω and 95Ω of SLGF at the middle of the line section. The simulation was carried out using the PSCAD version X4 to obtain the voltage of the faulty signal. The voltage was analyzed using a wavelet transform in MATLAB. The procedures were calculating the A_v and determining the ranking for all section. Finally the process of locating the fault was continued until the faulty section has been identified.

A. *Test of the Proposed Method*

To investigate the effectiveness of the proposed algorithm, fault impedance values of 75Ω, 85Ω and 95Ω were tested. The fault was applied at the middle of line section. After the fault was applied, there was a small fluctuation on the voltage signal. The fluctuation was hardly seen but after the image was zoomed as shown in Fig. 3(c), there was a small deviation on the signal. In order to illustrate the defect signal better, digital signal processing technique is necessary to analyze the signal. In this paper, wavelet transform was applied to examine the signal. After the signal was decomposed using the DWT-based MRA, sharp fluctuations on the detailed signal can be seen as shown in Fig. 3(d). This sharp variation depicts the time when the fault occurred.

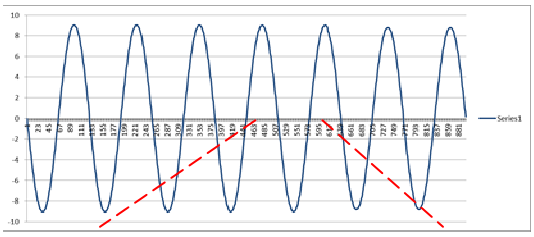

(a). Instantaneous voltage signal

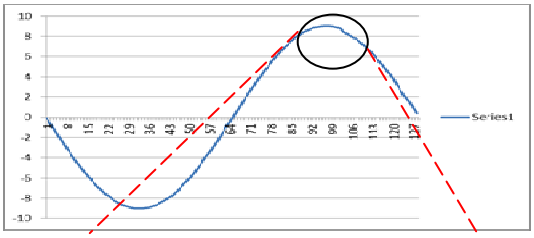

(b). 1st cycle of post-fault

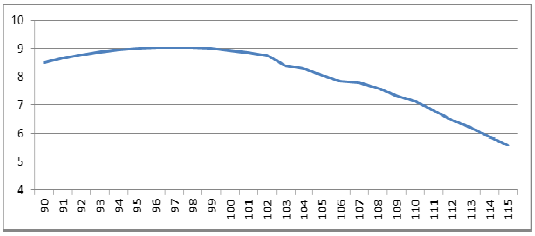

(c). Zoom in the fluctuation

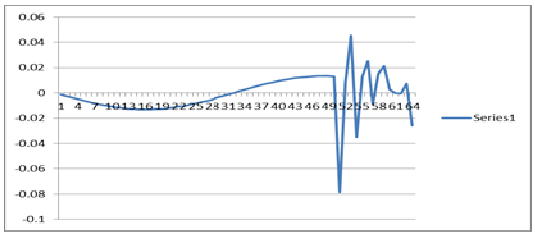

(d). Detail coefficients of wavelet transform
Fig. 3. HIF Detection on Voltage Signal.

The Fig. 4 and Fig. 5 show the first and second cycle of the post-disturbance voltage signal respectively. Both of the cycles were analyzed using the DWT-based MRA. After the signal was decomposed, 1st, 2nd and 3rd level of the detailed signal were obtained, as shown in the Fig. 4(b)-4(d) and Fig. 5(b)-5(d). The 1st level consists of 64 detailed coefficients sampled at 1.6-3.2 kHz frequency range. The 2nd and 3rd levels consist of 32 and 16 detailed coefficients sampled at 0.8-1.6kHz and 0.4-0.8kHz frequency range respectively. The detailed coefficients were summed up for each level and used for locating the faulty section.

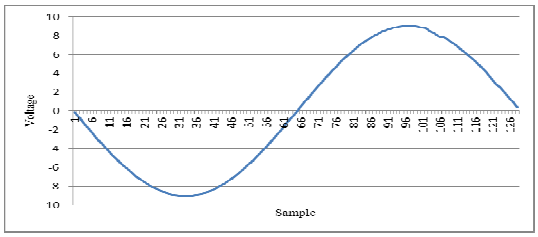

(a). 1st cycle of post-fault voltage signal.

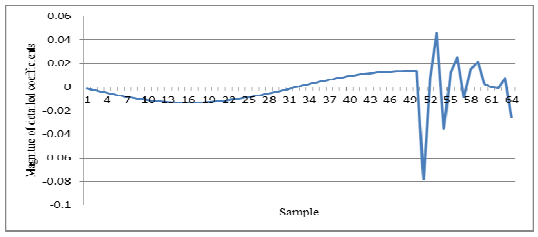

(b). 1st level of detail coefficients (∑d= 0.016476).

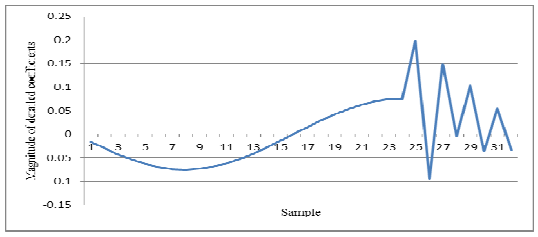

(c). 2nd level of detail coefficients (∑d= 0.157143).

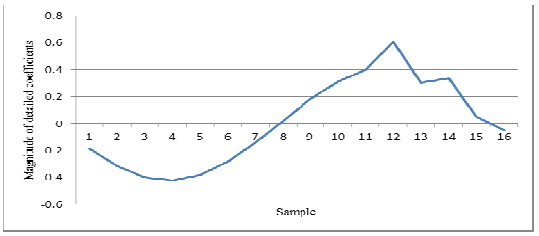

(d). 3rd level of detail coefficients (∑d= 1.587773).
Fig. 4. DWT based MRA Analysis for 1st Cycle of Voltage Signal.

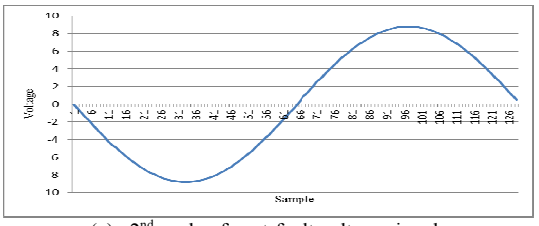

(a). 2nd cycle of post-fault voltage signal.

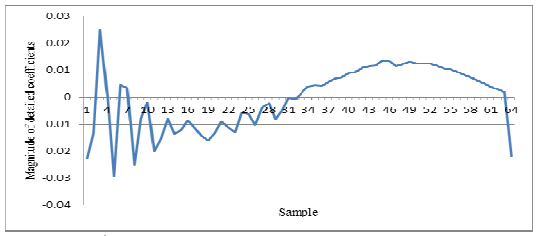

(b). 1st level of detail coefficients (∑d= 0.008644).

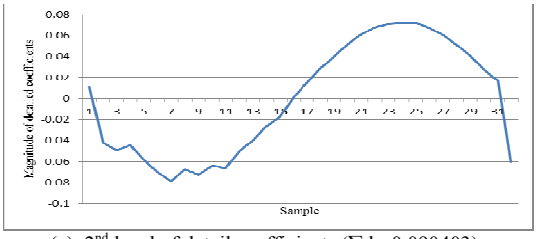

(c). 2nd level of detail coefficients (∑d= 0.090403).

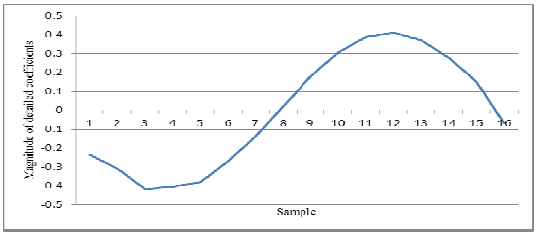

(d). 3rd level of detail coefficients (∑d= 1.411884).
Fig. 5. DWT based MRA Analysis for 2nd Cycle of Voltage Signal.

B. *Single Line to Ground Fault Analysis*

75Ω fault impedance is applied at the middle line of section 10. Table 1 shows the input data that are required for the simulation result to be compared with the databases for each level and phase. Referring to Table 2, the calculated average of absolute difference, AAD for each section shows that the lowest AAD of 75Ω SLGF impedance is in section 10. This indicates that the DWT-based MRA method is able to locate the faulty section correctly.

TABLE 1: DATA INPUT OF SUMMATION OF VOLTAGE DETAILED COEFFICIENTS FOR FAULT IMPEDANCE OF 75 Ω AT SECTION-10

Cycles	LEVEL 1			LEVEL 2			LEVEL 3		
	phase A	phase B	phase C	phase A	phase B	phase C	phase A	phase B	phase C
1st cycle	0.02107	0.01911	0.00907	0.17647	0.12279	0.09931	1.60607	1.43085	1.34539
2nd cycle	0.00796	0.00672	0.00695	0.09027	0.09370	0.09561	1.41283	1.46097	1.48735

TABLE 2: SIMULATION RESULTS FOR 75Ω, 85Ω AND 95Ω FAULT IMPEDANCE OF SLG

	75Ω at section 10		85Ω at section 23		95Ω at section 2	
Section	AAD	Ranking of AAD	AAD	Ranking of AAD	AAD	Ranking of AAD
1	0.00474	16	0.02438	19	0.00445	16
2	0.00272	7	0.02790	27	0.00144	2
3	0.00271	6	0.02822	33	0.00161	5
4	0.00307	12	0.02817	32	0.00193	10
5	0.00332	14	0.02814	31	0.00210	13
6	0.00267	5	0.02823	34	0.00158	4
7	0.00299	11	0.02813	30	0.00181	9
8	0.00279	8	0.02769	24	0.00156	3
9	0.00264	4	0.02771	25	0.00141	1
10	0.00243	1	0.02758	22	0.00164	6
11	0.00250	3	0.02753	20	0.00180	8
12	0.00283	10	0.02758	23	0.00202	11
13	0.00249	2	0.02755	21	0.00179	7
14	0.00281	9	0.02778	26	0.00202	12
15	0.00321	13	0.02799	28	0.00230	14
16	0.00354	15	0.02803	29	0.00251	15
17	0.03128	21	0.00153	3	0.02561	17
18	0.03165	22	0.00196	6	0.02587	18
19	0.03066	17	0.00159	4	0.02609	20
20	0.03069	18	0.00315	8	0.02680	21
21	0.03081	19	0.00343	9	0.02691	22
22	0.03086	20	0.00136	1	0.02595	19
23	0.03187	23	0.00144	2	0.02692	23
24	0.03340	24	0.00186	5	0.02818	24
25	0.03466	25	0.00309	7	0.02902	25
26	0.03533	28	0.00383	10	0.02961	26
27	0.03540	29	0.00391	11	0.02969	27
28	0.03575	31	0.00429	15	0.03004	28
29	0.03609	33	0.00467	17	0.03037	31
30	0.03616	34	0.00475	18	0.03041	32
31	0.03599	32	0.00457	16	0.03028	30
32	0.03560	30	0.00421	14	0.03018	29
33	0.03510	27	0.00393	12	0.03061	33
34	0.03493	26	0.00407	13	0.03071	34

*The circle shows the correct answer.

For 85Ω SLGF fault impedance in the middle of line section 23, the lowest AAD has been found in section 22 instead of section 23. In practice, when any fault occurs, engineers have to do a physical inspection by visiting the faulty location. Since the real fault does not occur at section 22, the section of the second lowest AAD is checked. It is found that the second lowest AAD is in section 23, where the real fault is located. Therefore, visual inspection in locating the actual fault based on the calculated AAD is able to locate the fault quickly.

95Ω SLGF fault impedance at the middle line of section 2 was simulated for further justification. It is found that, the faulty section is identified from the 2nd lowest AAD as shown

in Table 2. This is ensured that the proposed algorithm is also capable for locating the faulty section, at a branch section.

V. CONCLUSION

In this work, a discrete wavelet transform-based Multi-Resolution Analysis (MRA) has been adopted to locate the faulty section in a radial network of a typical distribution network in Malaysia. The 1st, 2nd and 3rd level resolution of detailed coefficients of voltage signals have been utilized. The faulty section was determined based on the smallest value of average of absolute difference, AAD between the measured signal and the database. The ranking of the AAD value is determined based on the lowest value to the highest value. A section with the lowest value of AAD is presumed to be the faulty section.

The proposed algorithm has successfully determined the faulty section based on the voltage signal. Since only two cycles of post-fault voltage signal is required, this method is capable of identifying the faulty section quickly. This method has also been found effective in locating the faulty section and is easy to be adopted in fault location.

VI. APPENDIX

I- LINE DATA OF RADIAL DISTRIBUTION NETWORK

Section	Node		Length (km)	Type of cable
	From	To		
1	3	4	1.254	A11UG300
2	4	14	1.29	A11UG185
3	14	17	0.5	A11UG185
4	17	18	0.5	A11UG185
5	18	19	0.25	A11UG300
6	14	15	0.395	A11UG185
7	15	16	0.51	A11UG185
8	4	5	0.14	A11UG185
9	5	6	0.4	A11UG185
10	6	7	0.35	A11UG185
11	7	12	0.3	A11UG300
12	12	13	0.75	A11UG300
13	7	8	0.2	A11UG300
14	8	9	0.5	A11UG300
15	9	10	0.27	A11UG300
16	10	11	0.5	A11UG300
17	20	34	0.5	A11UG240X
18	34	35	0.473	A11UG185
19	35	36	1.3	A11UG300
20	36	37	0.3	A11UG300
21	37	38	0.5	A11UG300
22	20	21	0.04	A11UG240X
23	21	22	0.884	A11UG185
24	22	23	0.54	A11UG185
25	23	24	0.716	A11UG240X
26	24	25	0.9	A11UG185
27	24	26	0.1	A11UG150X
28	26	27	0.5	A11UG185
29	27	28	0.723	A11UG185
30	28	29	0.45	A11UG185
31	27	30	0.594	A11UG185
32	30	31	0.908	A11UG185
33	31	32	0.5	A11UG185
34	32	33	0.5	A11UG185

II- CABLE PARAMETERS

Type Of Cable	Positive Sequence (pu/km)		Zero Sequence (pu/km)	
	R	X	R	X
A11UG300	0.12	0.0787	1.779	0.0396
A11UG185	0.195	0.0829	2.39	0.0406
A11UG240X	0.1609	0.1524	0.1814	0.0312
A11UG150X	0.2645	0.1603	0.2960	0.0352

VII. REFERENCES

[1] T. M. Lai, L. A. Snider, E. Lo, and D. Sutanto, "High-impedance fault detection using discrete wavelet transform and frequency range and RMS conversion," *IEEE Transactions on Power Delivery,* vol. 20, no. 1, pp. 397-407, 2005.

[2] A. H. Etemadi and M. Sanaye-Pasand, "High-impedance fault detection using multi-resolution signal decomposition and adaptive neural fuzzy inference system," *IET Generation, Transmission & Distribution*, vol. 2, no. 1, p. 110, 2008.

[3] M. Michalik, M. Lukowicz, W. Rebizant, S.-J. Lee, and S.-H. Kang, "Verification of the Wavelet-Based HIF Detecting Algorithm Performance in Solidly Grounded MV Networks," *IEEE Transactions on Power Delivery*, vol. 22, no. 4, pp. 2057-2064, 2007.

[4] S. Chen, "Feature Selection for Identification and Classification of Power Quality Disturbances", *Power Engineering Society General Meeting, Vol. 3, 2005*, pp. 2301-2306.

[5] S. Avdakovic and A. Nuhanovic, "Identifications and Monitoring of Power System Dynamics Based on the PMUs and Wavelet Technique," *Engineering and Technology*, pp. 796-803, 2010.

[6] P. K. Dash, B. K. Panigrahi, G. Panda, "Power Quality Analysis using S-transform", *IEEE Transactions on Power Delivery, vol. 18*, 2003, pp. 406-411.

[7] S. Suja, J. Jerome, "Pattern Recognition of Power Signal Disturbances using S-Transform and TT-Transform", *International Journal of Electrical Power & Energy Systems, vol. 32*, 2010, pp. 37-53.

[8] Z.-Y. Li, W.-l. Wu, "Classification of Power Quality Combined Disturbances Based on Phase Space Reconstruction and Support Vector Machines", *Journal of Zhejiang University - Science A vol. 9*, 2008, pp. 173-181.

[9] M. Sarlak and S. M. Shahrtash, "High impedance fault detection using combination of multi-layer perceptron neural networks based on multi-resolution morphological gradient features of current waveform," *IET Generation, Transmission & Distribution*, vol. 5, no. 5, p. 588, 2011.

[10] N. I. Elkalashy, M. Lehtonen, H. A. Darwish, A.-M. I. Taalab, and M. A. Izzularab, "A novel selectivity technique for high impedance arcing fault detection in compensated MV networks," *European Transactions on Electrical Power*, vol. 18, no. 4, pp. 344-363, 2008.

[11] N. I. Elkalashy, M. Lehtonen, H. A. Darwish, A.-M. I. Taalab, and M. A. Izzularab, "DWT-based extraction of residual currents throughout unearthed MV networks for detecting high-impedance faults due to leaning trees," *European Transactions on Electrical Power*, vol. 17, no. 6, pp. 597-614, 2007.